

COMPUTER SIMULATIONS OF A STOCHASTIC MODEL FOR THE NON-IMMUNE DISEASE SPREAD

© *Ilnytskyi Ja. , Holovatch Yu. , Kozitsky Yu. , Ilnytskyi H. , 2014*

We present a model of the non-immune disease spread, as well as an algorithmic approach and the corresponding results of its study by computer simulations. The model is a generalization of the *SIS* model with the uniform two-dimensional spatial distribution of individuals undergoing a Markov-type evolution with discrete time. In this work, we describe our approach and present a number of the preliminary results obtained for the case of the quenched distribution of individuals on the sites of a simple square lattice and the one-parameter stochastic dynamics (synchronous *SIS* model on a square lattice with varying number of neighbors). The dynamical properties of the model are studied in terms of the behavior of the fraction of the infected individuals as well as of the maximum size and dimension of the largest cluster formed by them. These properties are found to be affected by the effective range of the local infectivity, which demonstrates the role of the underlying graph of the individual communications on the global disease spread. The presented approach allows for numerous extensions, including the possibility to consider non-homogeneous spatial distributions and various forms of the stochastic dynamics.

Key words: epidemiology, computer simulations, *SIS* model, critical phenomena

1. Introduction

Since the seminal work by Kermack and McKendrick [1], modeling the disease spread had found much interest in both medical and applied mathematics circles (see, e.g. [2-3]). There are many ways the epidemiology models can be classified, therefore here we will restrict ourselves to discussing the features relevant to the purpose of this study. In deterministic models, the population is split into several large groups, the principal ones would be: fraction of susceptible to illness (S) and fraction of infected (I). If the individual develops an immunity to the disease after being cured (e.g. smallpox), it will move to the group of removed with their fraction R . This model is commonly abbreviated as *SIR* model. In the case of non-immune illness, cured individuals return back to S group, thus the *SIS* model. The definition of the model contains a set of transfer rules for the individuals to move between the groups. Diagrams for *SIS* and *SIR* models are depicted in Fig.1. As one can see, newborn individuals are joining group S with the rate π , whereas dying ones leave groups S and I with the rates μ and μ_I , respectively, β and γ are infecting and curing rates, respectively, reflecting the rate at which individuals move to and from group I . Note that the probability of the individual to be infected is proportional to the product of currently available susceptible and infected individuals SI . Normalization conditions $S + I = 1$ and $S + I + R = 1$ hold for *SIS* and *SIR* models, respectively.

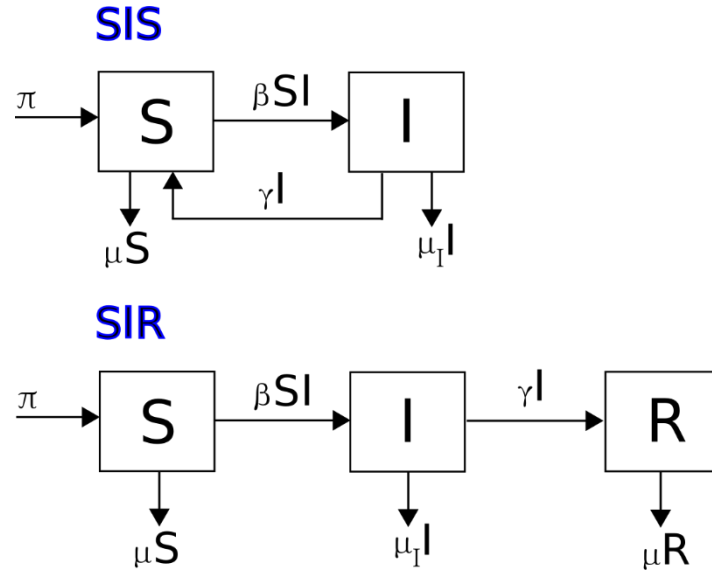


Fig.1. *SIS* and *SIR* deterministic models definitions. S , I and R are fractions of susceptible, infected and removed, respectively, flow rules are shown via arrows; π is birth rate, μ and μ_I are natural death rate and death rate for infected, respectively; β and γ are infecting and curing rates, respectively. $S + I = 1$ for *SIS* model and $S + I + R = 1$ for *SIR* model.

For the *SIS* model, the flow diagram of Fig. 1 is conveniently written as a set of first-order differential equations:

$$\begin{aligned}\frac{dS}{dt} &= \pi - \beta SI + \gamma I - \mu S \\ \frac{dI}{dt} &= \beta SI - \gamma I - \mu_I I\end{aligned}\tag{1}$$

As mentioned by Britton [5], “the type of questions that were addressed were for example: is it possible that there is a big outbreak infecting a positive fraction of the community? How many will get infected if the epidemic takes off? What are the effects of vaccinating a given community fraction prior to the arrival of the disease? What is the endemic level?” The ratio $R_0 = \beta/\gamma$ is of main importance here and it is usually referred to as the basic reproduction number for the infection. When $R_0 > 1$ the epidemic takes off and when $R_0 < 1$ there is no epidemic. The set of differential equations (1) can also be used to obtain a balance equation for the final state at $t \rightarrow \infty$. As these problems were resolved, the simple models were generalised in several ways towards making them more realistic. The examples of such generalisations are: introducing of an additional group of latently infected (E) for the case of diseases with long incubation period (e.g. tuberculosis [3]), splitting group S into several subgroups (e.g. low-risk and high-risk subgroups [3]), etc. Such extensions enable more flexibility for the simple deterministic models by tuning them to a particular type of the disease and particular environment of its spread.

However, the results obtained via employment of simple deterministic models, rely on the homogeneity of a community and on an assumption that individuals mix uniformly with each other. In this way, these models are of the mean-field type, using the terminology from the phase transitions [4]. Hence, another way of generalization of simple deterministic model is to study stochastic epidemic models [5]. These have also shown to be advantageous when the contact structure in the community contains small complete graphs: e.g. households and other local social networks. The details of an underlying network of human contacts, as shown by many examples in rapidly developed theory of complex networks [7], may bring the description of the disease spread into another level, as compared to structureless deterministic models. In this way we arrive to stochastic epidemic models which contain certain graph for human communication and stochastic dynamics for the infecting spread and cure defined via certain algorithm. Each individual in such model is treated as a single entity with several possible states (e.g. susceptible and infected) and connected to other individuals by means of a certain graph. The latter can be quenched or dynamically changed by means of bonds creation/destruction, individual jumps, etc. The infection spreads in a stochastic way, the same hold for curing of infected individuals. The dynamics is described as the Markovian process. In this way, the link to the simple deterministic model is provided via evaluation of S , I and R , the total number of susceptible,

infected and removed individuals, respectively. However, on a top of that, the spatial arrangement of clusters with infected individuals, distribution of their sizes and other local properties can also be studied. The influence of a local and global graph structure, as well as of possible individuals movement can be studied as well. In this study we consider computer simulation of one particular realization of a stochastic epidemic model, namely: *SIS* model on a two-dimensional square lattice. The details of the model, algorithmic solutions and results are presented in section 2. Conclusions are provided at the end of the study.

2. Model, algorithms and results

We consider *SIS* model on a two-dimensional square lattice of linear size L , hence total number of sites is $N = L^2$. Each i -th site contains one individual that is characterized by its state $s(i) = 0, 1$, where 0 stays for susceptible and 1 for infected. Individuals are assumed to be immobilized and can only change their state reacting on the state of their neighbours. The stochastic dynamics of the system is defined *via* the rules for changing the state of the individual i :

- if $s(i) = 0$ then it can switch to $s(i) = 1$ with the probability defined locally as $\beta n_I/q$, where n_I is the number of infected neighbours for site i , and q is the total number of its neighbours (coordination number of a lattice)
- if $s(i) = 1$ then it can switch to $s(i) = 0$ with constant probability γ

A link to simple deterministic *SIS* model, Eq.(1) can be established now. First of all, the infecting rate is proportional to β in both cases, but in the case of stochastic model it is a local quantity, being dependant on a number of infected neighbours n_I . The average value for n_I/q , however, will be equal to βI if one assumes that all individuals communicate one with another, providing a link to the deterministic model. Curing rate is constant in both models and equal to γ . In this study we will restrict ourselves to the case of synchronous *SIS* model, when $\beta = 1 - \gamma$. Its behaviour is governed by a single parameter, e.g. curing rate γ or $\lambda = \beta/\gamma = (1 - \gamma)/\gamma$ can be used equally. The latter parameter λ has a meaning of local reproduction ratio for the infection. The model is already considered for the case of the nearest neighbors only ($q = 4$ for the case of square lattice): it is called the contact process [8-10]. It exhibits phase transition with the critical behavior similar to that of the directed percolation [8-9].

In this study we consider a family of lattice stochastic *SIS* models with the condition $\beta = 1 - \gamma$ considered on a square lattice with various coordination number q . The latter is defined via a neighbours sphere of certain radius R_{nn} . In particular, at $R_{nn} = 1$, one obtains the nearest neighbours model with $q = 4$, at $R_{nn} = \sqrt{2}$ one has $q = 8$ and so on. We focus on critical behaviour of such models, which is governed by a local curing rate γ (λ being defined above can also be used). Several aspects of the critical behavior [4] are of the interest for us. First of all it is the influence of a finite system size L . Then, we are studying the effect of an increase of infection range, via variation of the R_{nn} value and, hence, the coordination number q . This effectively changes the connectivity of the underlying graph, on which the individuals reside. One expects to reproduce the critical behaviour of simple deterministic model in the limit of $R_{nn} \rightarrow \infty$. Finally, we would exploit the benefits of stochastic model by analysing the average and maximum cluster sizes of infected individuals and study them on a subject of percolation.

The workflow of the simulation algorithm is as follows:

1. The initial configuration is formed by creation of the simulation box of linear size L with $N = L^2$ individuals with their IDs numbered sequentially from 1 to N . The individuals are confined to the sites of a square lattice with lattice spacing equal to 1. Each site acquires initial status 1 with the probability p and status 0 with the probability $1 - p$, in most cases the value $p = 0.1$ was used.
2. The list of neighbors has been built for each individual according to the radius R_{nn} or the neighbors sphere and taking into account periodic boundary conditions [11]. Aiming on future extension of our study to the off-lattice models (with the continuous coordinates space) we used the general linked cells list algorithm used in molecular dynamics simulations of atomic systems [11,12]. To this end

the simulation box is split into square domains of linear size larger or equal to R_{nn} and the linked lists are built for each domain out of individuals IDs falling into this particular domain. Then, the pairs of adjacent domains are analyzed for the neighbors within the distance of R_{nn} and the neighbour lists are saved. Computing resources required to build neighbour lists using this algorithm scale as N at large N , in contrary to $N(N-1)/2$ for simple loop over all pairs in the simulation box.

3. The infecting/curing sweep over the system is performed. The sweep contains N attempts to pick an individual randomly. If the individual is infected than it is cured with the probability γ and it transmits the infection to one of its neighbours with the probability $1 - \gamma$. To do so one generates a random number θ evenly distributed within an interval $[0,1]$. If $\theta < \gamma$ then the status of selected individual changes from 1 to 0 (curing takes place), otherwise the status of one of its randomly selected neighbours changes from 0 to 1 (infecting of a neighbour takes place).
4. The clusters of infected individuals are identified using efficient Hoshen-Kopelman algorithm [13]. Initially each infected individual is assigned a cluster label that coincides with its ID. The sweeps over the neighbors pairs using the linked cells lists (introduced in step 2) are performed and cluster labels reduction takes place for the neighboring individuals, the process continue until no reductions occur. At the end each individual is assigned the label that identifies its host cluster.
5. The properties of interest are evaluated such as fraction of infected individuals, average and maximum cluster sizes, search for percolating clusters. The accumulators for average properties are updated.
6. Go back to step 3 until desired number of sweeps is performed.

First we consider the case of $q = 4$ model (square lattice with disease spread over nearest neighbours only). For this model we performed simulations for various linear system sizes ranging from $L = 16$ to 512 with the periodic boundary conditions being applied. For each system size the interval of values for curing rate from $\gamma = 0.005$ to $\gamma = 0.7$ is covered with the step of 0.005, and for each pair $\{L, \gamma\}$ 5000 sweeps were performed. The system was found in a stationary state with saturated value of I pretty fast, typically after up to 100 sweeps. The evolution of I during first 100 sweeps is illustrated in Fig.2 for two system sizes, $L = 32$ and 256, and a few characteristic values of the curing rate γ . The time unit is set equal to one sweep over the system.

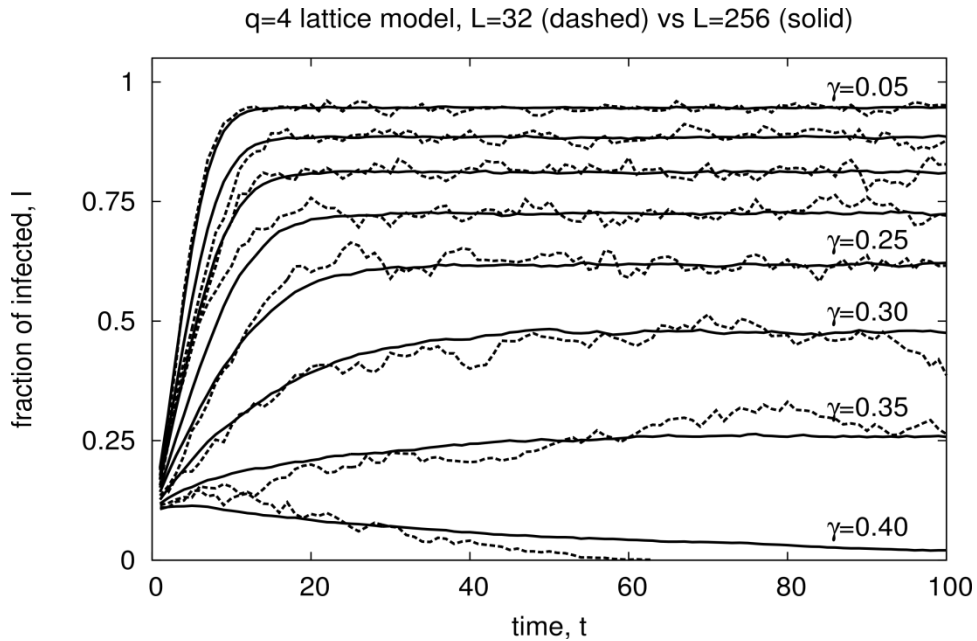


Fig.2. Evolution of the fraction of infected individuals I towards a stationary state for the $q = 4$ model of

system sizes $L = 32$ (shown as dashed lines) and $L = 256$ (solid lines) at various curing rate γ .

One can see an essential increase of the time needed to reach stationary state when curing rate approaches the interval of values $\gamma = 0.3 - 0.4$. However, there is no evidence for the system size dependence, as the curves built for $L = 32$ and $L = 256$ at the same γ exhibit essentially the same shape with only more fluctuations being evident for the smaller system size of the two. Obviously, small values of curing rate γ lead to the $I = 1$ stationary state (all are infected) whereas with an increase of γ one observes that fraction of infected individuals vanishes in time starting from the ‘critical’ value of $\gamma \approx 0.4$. This is further outlined in Fig. 3 as described below.

Let us examine the fraction of infected individuals in a stationary state I vs curing rate γ for the same model. The data are shown in Fig.3 and there is a clear evidence for a continuous transition from the state with $I \approx 0$ and $I > 0$ that occurs at certain critical value γ_c (see, e.g. [9]). Therefore the data can be fitted to the following power form:

$$I = A(\gamma_c - \gamma)^{\beta'}$$

where β' is the critical exponent for the order parameter [4], which in this case is I . Fitting of data is performed via the built-in routine of plotting program *gnuplot* that uses the least-squares method. The results of the fit are displayed in Fig.3. First of all let us remark that, again, we found no system size dependence as all the data obtained at various system sizes fit to practically the same master curve. The value for critical curing rate $\gamma_c \approx 0.3762$ is very close to the estimate $\gamma \approx 0.3775$ made for the contact process [9,10], whereas the critical exponent has a mean-field value $\beta' \approx 0.5$.

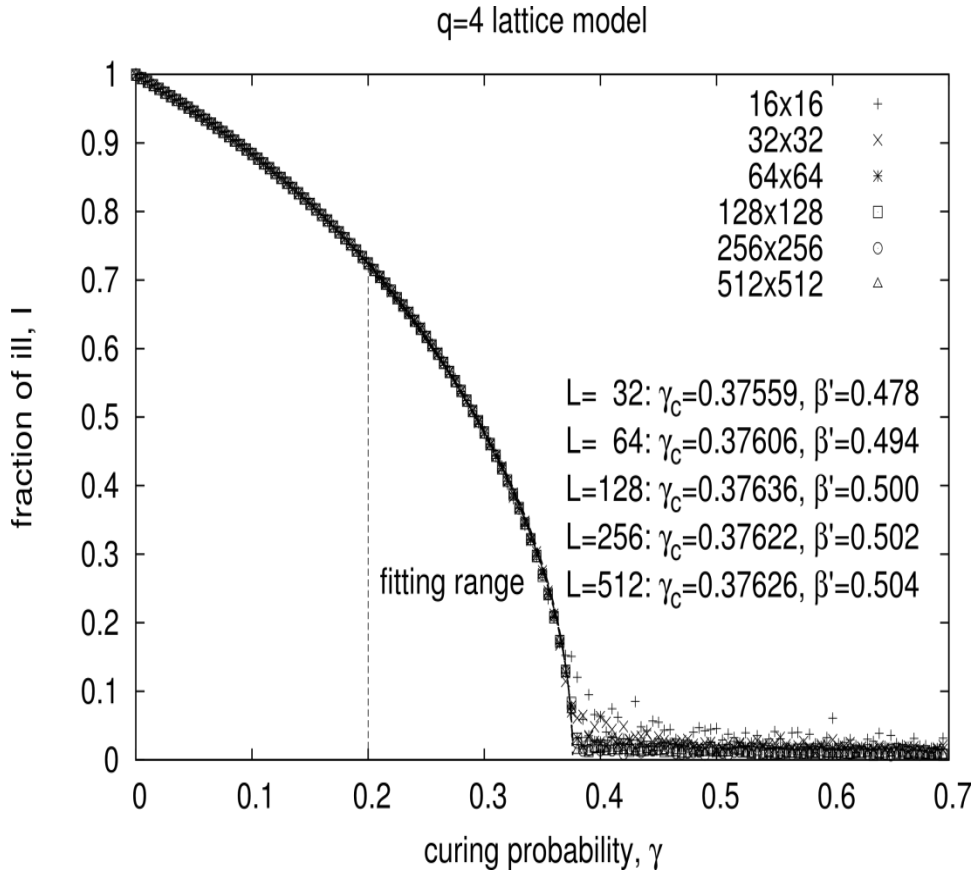


Fig.3. Fraction of infected individuals I in the stationary state vs curing rate γ for the $q = 4$ model of system sizes $L = 16 - 512$. Fitted parameters β' and γ_c are shown in the plot.

Now we will switch to the more general case of the lattice model with the values of q other than 4 (this can be achieved by choosing appropriate value for the radius R_{nn} for neighbors sphere, as remarked above). By doing so we increase the effective range of the disease spread from infected individual to susceptible ones that surround it. If R_{nn} is of the range of $L/2$ then the model is reduced to the deterministic *SIS* model, Eq.(1). In this case all individuals are bonded one with another and the model is reduced to a mean-field type system. The simulation algorithm discussed above is inefficient in this case, as far as the computing time expenditure is proportional to N^2 (due to the fact that the neighbor lists for each individual include all the other individuals). Therefore step 2 of the algorithm is omitted and step 3 is simplified in a way that each infected individual infects with the probability $(1 - \gamma)I$ any other random individual in a system. The local reproduction number $\lambda = \beta/\gamma = (1 - \gamma)/\gamma$ reduces itself to its global counterpart R_0 in this case. The latter has its critical value at $R_0 = 1$. Therefore, the critical value for γ_c is expected to be equal to $\gamma_c = 1/(\lambda_c + 1) = 1/(R_0 + 1) = 0.5$. This is found indeed to be a case, as is indicated in Fig.4, where the fraction of infected individuals I vs curing rate γ is shown for the cases of $q = 4, 8, 12, 20$ and for the case when all particles interact one with another, denoted as 'q=all'. In the latter case γ_c is found to be very close to 0.5 (see, Fig.4). The critical exponent β' is found to be dependant on the effective range of interaction q , approaching value close to $3/4$ in the limiting case of $q=\text{all}$.

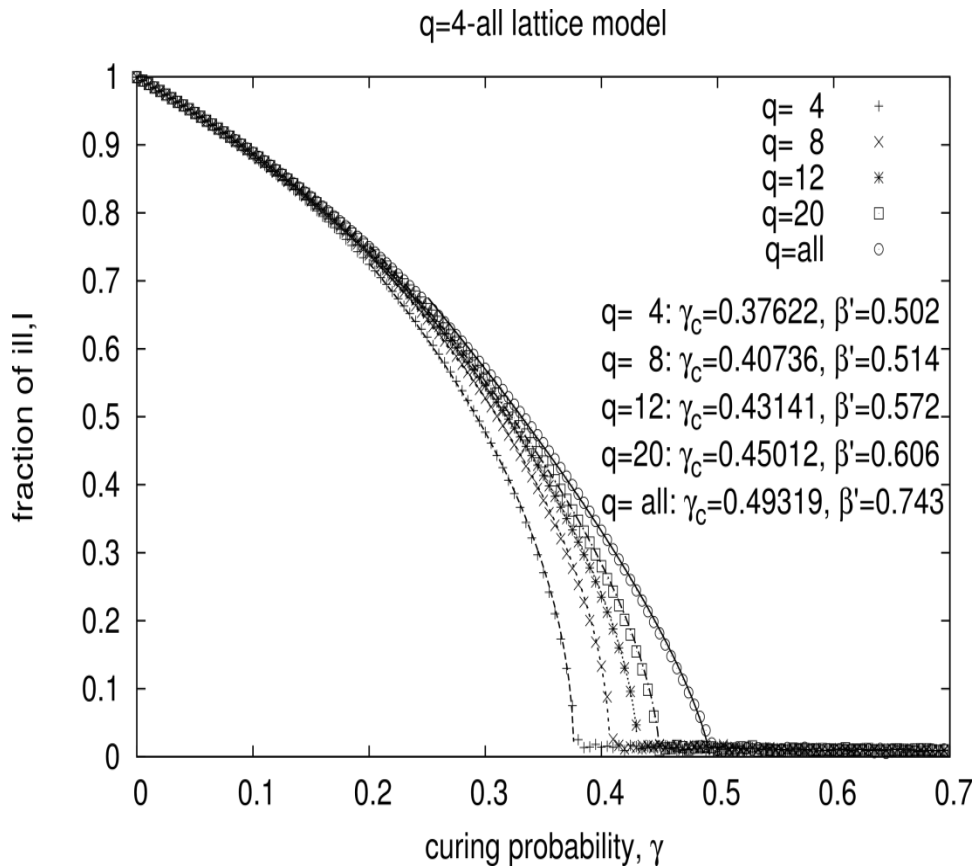


Fig.4. The same as Fig.3 but for the generalized model with various q ($q=\text{all}$ is for the limit). Linear system size is $L = 256$.

Let us now turn our attention to the effects of clustering for the infected individuals. Their spatial distribution within the simulation box can be monitored via snapshots, where infected individuals are shown in black, whereas susceptible are not shown. Fig.5 contains such snapshots for the $q = 4$ model of linear size $L = 256$ studied at curing rate $\gamma = 0.3$ and monitored at time instances $t = 0, 20$ and 80 . The initial system (at $t = 0$) is homogeneous, whereas an evident clustering takes place as the system moves towards the stationary state.

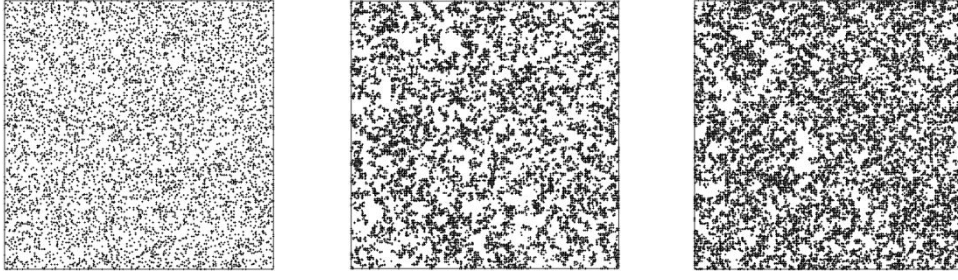


Fig.5. Snapshots illustrating state of the system of linear size $L = 256$ and curing rate $\gamma = 0.35$ while reaching the stationary state. Time instances $t = 0$ (image on the left), $t = 20$ (image in the middle) and $t = 80$ (image on the right) are shown. Infected individuals are shown in black, susceptible ones are not shown. See also Fig.2 for the reference.

To quantify the clustering effects we introduce such properties as scaled average cluster size $\langle n_c \rangle = \langle N_c \rangle / N$ here N_c denotes cluster sizes in number of individuals, averaging is performed over all clusters in the system), scaled maximum cluster size $n_{c,max} = N_{c,max} / N$ ($N_{c,max}$ is the number of particles in the largest cluster in the system) and scaled maximum cluster dimension $l_{max} = \max\{L_x, L_y\} / L$, where L_x, L_y is maximum span of the cluster along X and Y axis, respectively. The latter property serves as an indicator for the percolation, which takes place if $l_{max} \approx 1$. Behaviour of the average cluster size indicates strong system size, as is seen in Fig.6. Shift of the curve towards left side is a consequence of the fact that a larger number of small clusters appear in larger system, resulting in both lowering their scaled sizes and reducing the average value.

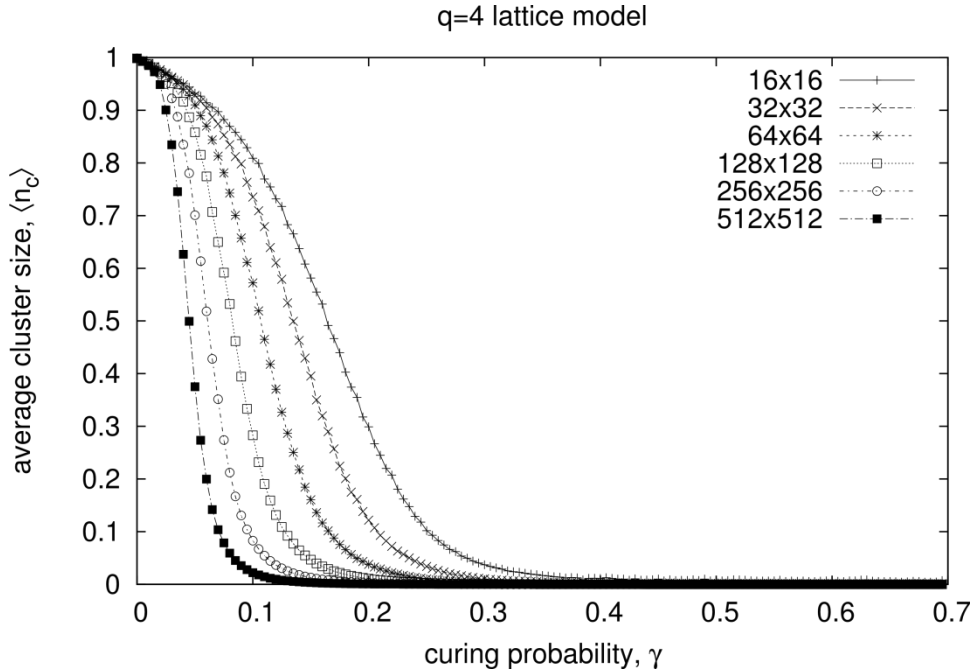


Fig.6. The average cluster size vs γ for $q = 4$ and various system sizes $L = 16 - 512$ indicated in the plot.

The behavior of both maximum cluster size (Fig.7) and maximum cluster dimension (Fig.8) indicate the presence of another transition which takes place at $\gamma = 0.27$. The plot for the maximum cluster dimension (Fig.8) indicate the existence of the percolation transition exactly at the same value $\gamma = 0.27$. The curves

drop down abruptly at $\gamma = 0.27$ and the effect is more pronounced for larger system sizes. The details of both transitions requires more thorough analysis and, possibly, application of more sophisticated techniques applicable near the phase transition point. As one knows, in this region the system is subject to slow relaxation and both longer runs and special algorithms should be applied. This, as well as generalized models with various types of connecting graphs, are reserved for future publications.

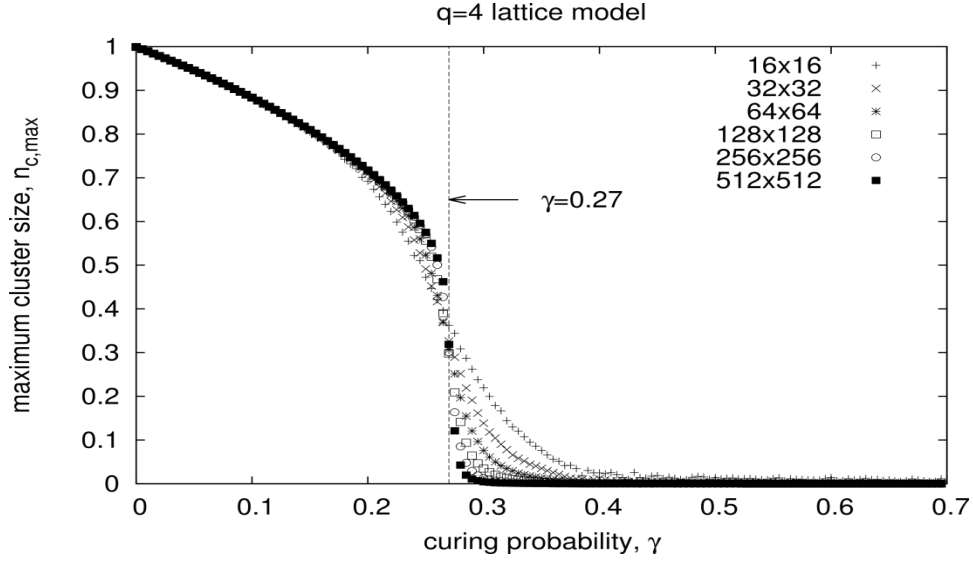


Fig.7. The maximum cluster size vs γ for $q = 4$ and various system sizes $L = 16 - 512$ indicated in the plot.

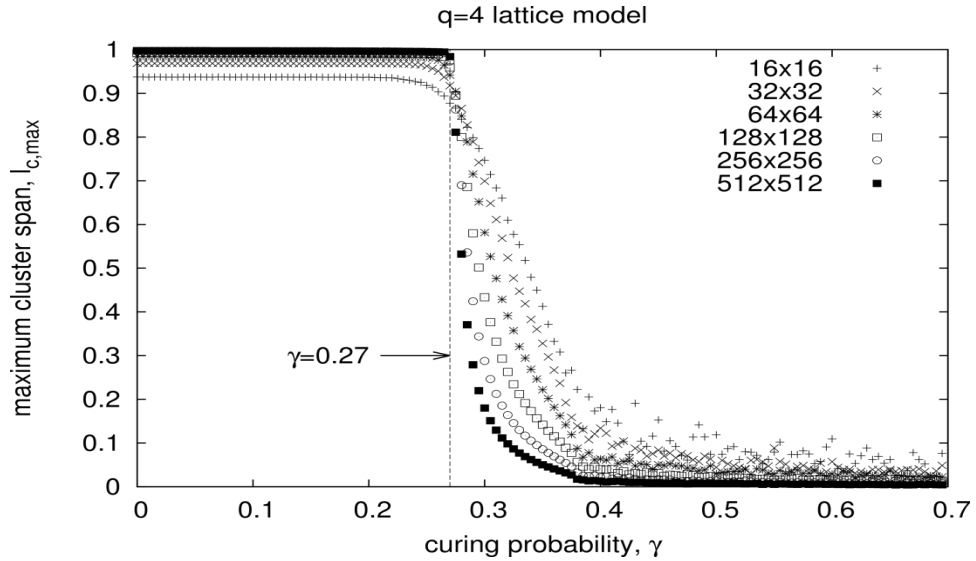


Fig.8. The maximum cluster dimension l_{max} vs γ for $q = 4$ and various system sizes $L = 16 - 512$ indicated in the plot.

3. Conclusions

In this paper, we have presented results of computer simulations of a stochastic model for study of non-immune disease spread. In models of this type, the point at which an epidemic occurs corresponds to the percolation probability at which a giant component of connected nodes first forms. In addition to study static behavior of a system in vicinity of this point (which corresponds to percolation), one also analyzes dynamics

of disease spread and a non-equilibrium phase transition which is typical for the disease-spreading models. Our results bring about the influence of the details of microscopic structure and local infective dynamics to the spread of non-immune disease. We reproduced the known critical behavior of contact process and extended the study to the case of variable range of infecting. It is found that the percolation transition is followed by complete dying out of the disease at larger value of curing probability. In-between two transition system is split into clusters of infected individuals with their dimensions much smaller than the system size.

With the above results at hand, we are in position to introduce several features modifying the model and making it closer to the real-world situations. On the one hand, work under progress is targeted on the off-lattice case, on the asymmetric model with adjustable both local curing and infecting rates independently, as well as including stochastic jumps of individuals. On the other hand, the delayed infecting and curing can be studied, matching the real dynamics of tuberculosis. In the latter case the statistical data available for Ukraine will be used. We also plan to consider the model, keeping its geographical embedding effects, on the scale-free small world network [7]. The latter are much closer to human social networks and have already served as a good testing ground for analysis of epidemic spreading [14].

Acknowledgement

This work was supported by the International Research Staff Exchange Scheme grant “Structure and Evolution of Complex Systems with Applications in Physics and Life Sciences” STREVCOMS-612669 within the 7th European Community Framework Program.

1. W.O. Kermack, A.G. McKendrick, *A contribution to the mathematical theory of epidemics*, *Proc. Roy. Soc. Lond. A* **115** (1927) 700.
2. F. Brauer, *The Kermack–McKendrick epidemic model revisited*, *Math. Biosci.* **198** (2005) 119–131.
3. C. Ozcaglara, A. Shabbeera, S.L. Vandenbergc, B. Yenera, and K.P. Bennetta, *Epidemiological models of Mycobacterium tuberculosis complex infections*, *Math. Biosci.* **236**(2) (2012) 77–96; Z. Hu , Z. Teng , H. Jiang, *Stability analysis in a class of discrete SIRS epidemic models*, *Nonlinear Analysis: Real World Applications* **13** (2012) 2017–2033.
4. See e.g. C. Domb, *The Critical Point*. (Taylor & Francis, London, 1996); Yu. Holovatch (Ed.). *Order, Disorder and Criticality. Advanced Problems of Phase Transition Theory*, vol. **1** (World Scientific, Singapore, 2004); vol. **2** (World Scientific, Singapore, 2007); vol. **3** (World Scientific, Singapore, 2012).
5. T. Britton, *Stochastic epidemic models: A survey*, *Mathematical Biosciences* **225** (2010) 24–35.
6. R.I. Hickson, G.N. Mercer, K.M. Lokuge, *A Metapopulation Model of Tuberculosis Transmission with a Case Study from High to Low Burden Areas*, *PLoS ONE* **7**(4) (2012) e34411.
7. See e.g. R. Albert, A.-L. Barabási, *Statistical mechanics of complex networks*. *Rev. Mod. Phys.* **74** (2002) 47–97; M. E. J. Newman, *The structure and function of complex networks*. *SIAM Review* **45** (2003) 167–256; S. Boccaletti, V. Latora, Y. Moreno, M. Chavez, D.-U. Hwang, *Complex networks: Structure and dynamics*. *Physics Reports* **424** (2006) 175–308; Yu. Holovatch, O. Olemskoi, C. von Ferber, T. Holovatch, O. Mryglod, I. Olemskoi, V. Palchykov, *Complex networks*. *J.Phys.Stud.* **10** (2006) 247–289.
8. P. Grassberger and A. de la Torre, *Reggeon field theory (Schlögl's first model) on a lattice: Monte Carlo calculations of critical behaviour*, *Ann. Phys. (N.Y.)* **122** (1979) 373.
9. A.G. Moreira, R. Dickman, *Critical dynamics of the contact process with quenched disorder*, *Phys. Rev. E* **54** (1996) R3090–3093.
10. M.M.S. Sabag and M.J. de Oliveira, *Conserved contact process in one to five dimensions*. *Phys. Rev. E* **66** (2002) 036115.
11. D.C. Rapaport, *The Art of Molecular Dynamics Simulation*, Cambridge University Press; 2 edition (2004), 564p.
12. J.M. Ilnytskyi, M.R. Wilson, *A domain decomposition molecular dynamics program for the simulation of flexible molecules with an arbitrary topology of Lennard–Jones and/or Gay–Berne sites*, *Comp. Phys. Commun.* **134** (2001) 23–32.
13. J. Hoshen and R. Kopelman, *Percolation and cluster distribution. I. Cluster multiple labeling technique and critical concentration algorithm*, *Phys. Rev. B* **14**, (1976) 3438.
14. R. Pastor-Satorras, A. Vespignani, *Epidemic Spreading in Scale-Free Networks*. *Phys. Rev. Lett.* **86** (2001) 3200–3203;
15. M. E. J. Newman, D. J. Watts, *Scaling and percolation in the small-world network model*. *Phys. Rev. E* **60** (1999) 7332–7342;
16. C. Moore, M. E. J. Newman, *Epidemics and percolation in small-world networks*. *Phys. Rev. E* **61** (2000) 5678–5682;
17. Y. Moreno, R. Pastor-Satorras, A. Vespignani, *Epidemic outbreaks in complex heterogeneous networks* *Eur. Phys. Journ. B* **26** (2002) 521;
18. M. E. J. Newman, *Spread of epidemic disease on networks*. *Phys. Rev. E* **66** (2002) 016128.